Electrostatic Comb Drive Levitation and Control Method

William C. Tang, *Member, IEEE*, Martin G. Lim, and Roger T. Howe, *Member, IEEE*

Abstract—**This paper presents the theory, simulation results, and experimental study of the levitating force (*normal* to the substrate) associated with interdigitated capacitor (electrostatic comb) lateral actuators. For compliant suspensions, normal displacements of over 2 μm for a comb bias of 30 V are observed. This phenomenon is due to electrostatic attraction induced on top of the suspended structure. By electrically isolating alternating drive-comb fingers and applying voltages of equal magnitude and opposite sign, levitation force can be reduced by an order of magnitude, while reducing the lateral drive force by less than a factor of 2. The levitation theory incorporates electrostatic simulation results, and agrees well with experimental data.**

I. Introduction

SURFACE-MICROMACHINED polysilicon resonators which are driven by interdigitated capacitors (electrostatic combs) have several attractive properties (Fig. 1) [1]–[4]. Vibrational amplitudes of over 10 μm are possible with relatively high quality factors at atmospheric pressure, in contrast to structures which move normal to the surface of the substrate. The comb-drive capacitance is linear with displacement, resulting in an electrostatic drive force which is independent of vibrational amplitude. Electrostatic combs have recently been used for the static actuation of friction test structures [5], microgrippers [6], and force-balanced accelerometers [7].

Potential applications of lateral resonators include resonant accelerometers and rate gyroscopes, as well as resonant microactuators [8]. For efficient mechanical coupling between a vibrating pawl and a toothed wheel, it is essential that both structures remain coplanar. However, 2-μm-thick polysilicon resonators with compliant folded-beam suspensions have been observed to levitate over 2 μm when driven by an electrostatic comb biased with a dc voltage of 30 V. This effect must be understood in order to design functioning resonant microactuators, with the possibility that levitation by interdigitated combs may offer a convenient means for selective pawl engagement.

Manuscript received May 20, 1992; revised November 13, 1992. This work was supported by the Berkeley Sensor & Actuator Center, an NSF/Industry/University Cooperative Research Center. Subject Editor, K. Petersen.

W. C. Tang is with the Ford Research Laboratory, Ford Motor Company, Dearborn, MI 48121.

M. G. Lim is with the Xerox Palo Alto Research Center, Palo Alto, CA 94304.

R. T. Howe is with the Department of Electrical Engineering and Computer Sciences, University of California at Berkeley, Berkeley, CA 94720.

IEEE Log Number 9206696.

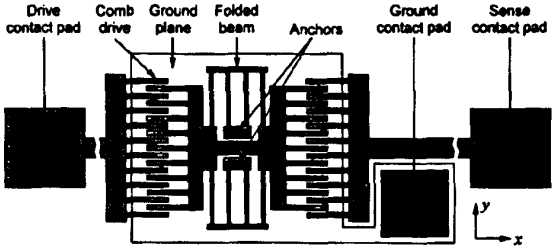

Fig. 1. Layout of a linear lateral resonator driven and sensed with interdigitated capacitors (electrostatic combs).

In this paper, the theory of electrostatic levitation is described along with the 2-D simulation results, which are then compared with experimental measurements of the reduction in levitation effect for the modified comb design with independently biased fingers.

II. Vertical Levitation Theory

A. DC Levitation

Successful electrostatic actuation of micromechanical structures requires a ground plane under the structure in order to shield it from relatively large vertical fields [9], [10]. It has been observed that if the underlying nitride and oxide passivation layers are not covered with a grounded polysilicon shield, the application of a dc bias voltage will cause the structures to be stuck down to the substrate. Furthermore, varying the bias voltage causes the structures to behave unpredictably. In previous studies of the electrostatic-comb drive, a heavily doped polysilicon film underlies the resonator and the comb structure. However, this ground plane contributes to an unbalanced electrostatic field distribution, as shown in Fig. 2 [11]. The imbalance in the field distribution results in a net vertical force induced on the movable comb fingers, which levitates the structure away from the substrate. Whether this force causes significant static displacement or excites a vibrational mode of the structure depends on the compliance of the suspension and the quality factor for vertical displacements.

Using a 2-D electrostatic simulation program (Maxwell Solver [11]) to simulate the cross section of the comb finger biased with a dc voltage, we obtain the induced vertical force per unit length of the movable comb finger at different levitation positions. This vertical force density, F_{z0} [nN·μm^{-1}], is then plotted against levitation, z [μm],

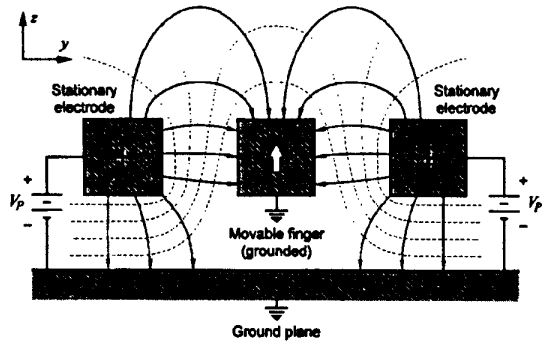

Fig. 2. Cross section of the potential contours (dashed lines) and the electric fields (solid lines) of a comb finger under levitation force induced by two adjacent electrodes biased at a positive potential.

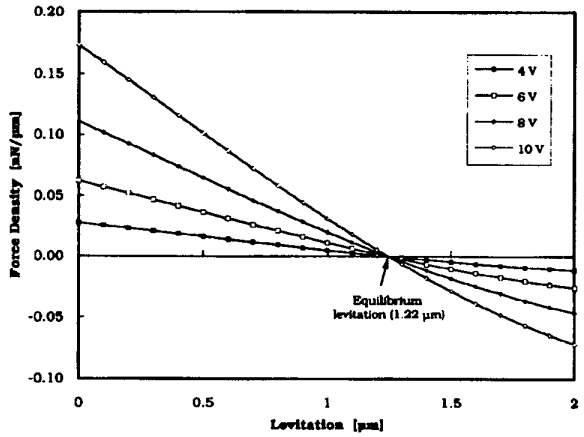

Fig. 3. Simulated levitation force density versus vertical position under different biasing voltages. Finger dimensions are 2 μm thick × 4 μm wide; nominal separations from the substrate and the drive electrodes are 2 μm.

at different dc bias voltages, V_p [V]. Fig. 3 is the simulation results of a 4-μm-wide × 2-μm-thick comb finger excited by two identically sized electrodes situated 2 μm away from both sides of the finger, and 2 μm above a grounded substrate. There are several important observations from this simulation. First, the stable equilibrium levitation, z_0 (1.22 μm for this case), is the same for any nonzero bias voltages. Thus, in the absence of a restoring spring force, the movable comb fingers will be levitated to z_0 upon the application of a dc bias. Second, given z, F_{z0} is proportional to the square of the applied dc bias, V_P^2. And at any V_p, F_{z0} is roughly proportional to $(z_0 - z)$ as long as z is less than z_0. Thus

$$F_{z0} \propto V_P^2 \frac{(z_0 - z)}{z_0} \Rightarrow$$

$$F_{z0} \approx \gamma_{z0} V_P^2 \frac{(z_0 - z)}{z_0} \text{ for } z < z_0, \tag{1}$$

where the constant of proportionality, γ_{z0} (1.73×10^{-3} nN·μm^{-1}·V^{-2} for this case), is defined as the vertical drive capacity per unit length. If Δx is the comb-finger-overlap length, then the levitation force is given by $F_z = F_{z0}\Delta x$ and the vertical drive capacity, $\gamma_z = \gamma_{z0}\Delta x$. Equation (1) can then be rewritten as

$$F_z \approx \gamma_z V_P^2 \frac{(z_0 - z)}{z_0}. \tag{2}$$

This equation implies that since $F_z \propto (z_0 - z)$, the levitation force behaves like an *electrostatic spring*, such that $F_z = k_e(z_0 - z)$, where k_e is the electrostatic spring constant,

$$k_e = \frac{\gamma_z}{z_0} V_P^2. \tag{3}$$

Both (2) and (3) will be used extensively in the following discussions on vertical transfer function and vertical resonance.

B. Vertical Transfer Function

The total vertical force acting on the comb fingers includes the levitation force, F_z, and the passive restoring spring force, F_k, generated by the mechanical suspensions of the system, as illustrated in Fig. 4. The vertical dc transfer characteristics can be evaluated by solving

$$F_{net} = F_z - F_k = 0, \tag{4}$$

where F_{net} is the net force acting on the movable comb finger, and

$$F_k = k_z z, \tag{5}$$

where k_z is the vertical spring constant. Substituting (2) and (5) into (4), we have

$$\gamma_z V_P^2 \frac{(z_0 - z)}{z_0} - k_z z = 0. \tag{6}$$

Solving for z in terms of V_P yields

$$z = \frac{z_0 \gamma_z V_P^2}{k_z z_0 + \gamma_z V_P^2}. \tag{7}$$

Figure 5 is a plot of this equation by assuming a value of 86 nN·μm^{-1} for k_z [see (27)] and 720 μm for Δx to yield a value of 1.25 nN·V^{-2} for γ_z (18 fingers on each of the two comb drives and a 20 μm finger overlap). The initial slope of the curve is largely dependent on γ_z, which determines the threshold voltage where levitation reaches 90% of the maximum, and the asymptotic value approaches z_0. Therefore, in certain applications where vertical levitation is undesirable, both γ_z (which can be interpreted as the sensitivity of levitation to the applied voltage) and z_0 (the equilibrium levitation in the absence of returning spring force) should be minimized. The method to control vertical levitation is discussed later in this paper.

C. Vertical Resonant Frequency

In this subsection, we consider the case where the resonators are not damped vertically, such as for the case of vibrations in vacuum. In the absence of damping, the

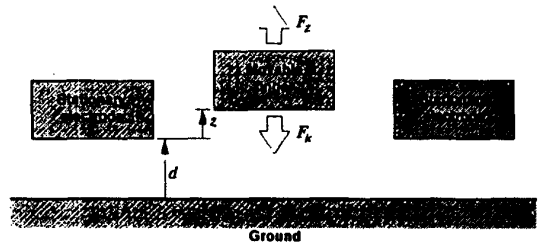

Fig. 4. The vertical forces acting on a movable comb finger.

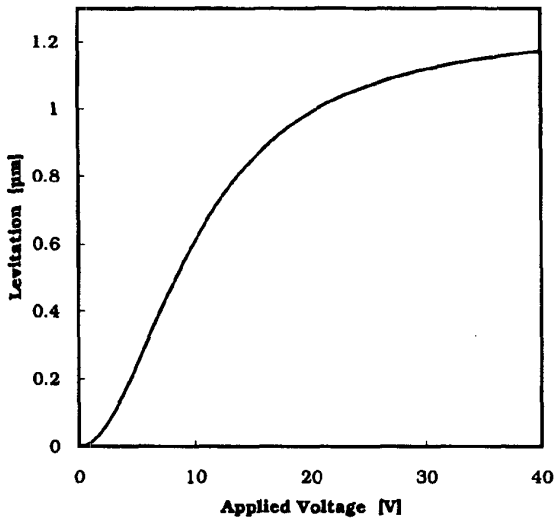

Fig. 5. Theoretical levitation (z) versus dc bias (V_P) based on (7), with $\gamma_z = 1.25\ \text{nN}\cdot\text{V}^{-2}$, $k_z = 86\ \text{nN}\cdot\mu\text{m}^{-1}$, and $z_0 = 1.22\ \mu\text{m}$.

governing equation of motion is a second-order differential equation given by

$$F_{\text{net}} = M\frac{d^2z}{dt^2}, \tag{8}$$

where M is the effective mass of the vibrating structure. The net vertical force, F_{net}, which is zero in dc analysis [eq. (4)], is now nonzero when the bias voltage, V_P, is replaced with a generalized, time-varying drive voltage, $v_D(t)$:

$$F_{\text{net}}(t) = F_z(t) - F_k(t) = \gamma_z\frac{[z_0 - z(t)]}{z_0}v_D^2(t) - k_z z(t). \tag{9}$$

This relationship can be linearized by assuming that $v_D(t) = V_P + v_d(t)$ and $z(t) = Z_P + z_d(t)$, where $V_P >> v_d(t)$ and $Z_P >> z_d(t)$. It is further assumed that $v_D(t)$ and $z(t)$ are continuously differentiable. Expanding F_z in a Taylor series about the operating point (V_P, Z_P) and retaining only the linear terms yields

$$F_z(v_D, z) \approx F_z|_{V_P,Z_P} + \frac{\partial F_z}{\partial v_D}\bigg|_{V_P,Z_P} v_d(t) + \frac{\partial F_z}{\partial z}\bigg|_{V_P,Z_P} z_d(t). \tag{10}$$

Carrying out the indicated operations yields

$$F_z(v_D, z) \approx \gamma_z\frac{(z_0 - Z_P)}{z_0}V_P^2 + 2\gamma_z\frac{(z_0 - Z_P)}{z_0} \cdot V_P v_d(t) - \frac{\gamma_z V_P^2}{z_0}z_d(t). \tag{11}$$

Substituting this result and (5) for F_k into (8) yields

$$\gamma_z\frac{(z_0 - Z_P)}{z_0}V_P^2 + 2\gamma_z\frac{(z_0 - Z_P)}{z_0}V_P v_d(t) - \frac{\gamma_z V_P^2}{z_0}z_d(t) - k_z[Z_P + z_d(t)] = M\frac{d^2[Z_P + z_d(t)]}{dt^2}. \tag{12}$$

Since Z_p is constant, $(dZ_P/dt) = 0$. Further, in the light of (6), the dc terms cancel, yielding

$$Gv_d(t) = M\frac{d^2z_d(t)}{dt^2} + k_{eq}z_d(t), \tag{13}$$

where

$$G = 2\gamma_z\frac{(z_0 - Z_P)}{z_0}V_P \quad [\text{nN}\cdot\text{V}^{-1}] \tag{14}$$

and

$$k_{eq} = k_e + k_z \quad [\text{nN}\cdot\mu\text{m}^{-1}], \tag{15}$$

with k_e as defined in (3). Equation (13) describes an undamped oscillator with drive $v_d(t)$. The system has a resonant frequency

$$\omega_1 = \left(\frac{k_e + k_z}{M}\right)^{1/2}. \tag{16}$$

An important observation is that the resonant frequency is a strong function of the applied bias, V_P. If we define the mechanical resonant frequency (under zero bias) as ω_0, then

$$\frac{\omega_1}{\omega_0} = \left(\frac{k_e + k_z}{k_z}\right)^{1/2} = \left(\frac{k_z + \frac{\gamma_z}{z_0}V_P^2}{k_z}\right)^{1/2}, \tag{17}$$

which is plotted in Fig. 6 as a function of V_P. In the limit as $V_P \to \infty$,

$$\lim_{V_P\to\infty}\left(\frac{\omega_1}{\omega_0}\right) = \left(\frac{\gamma_z}{z_0 k_z}\right)^{1/2}V_P. \tag{18}$$

If we further assume that the input drive $v_d(t)$ is sinusoidal, e.g., $v_d(t) = A\sin(\omega t)$, then the resulting output is given by

$$z_d(t) = B\sin(\omega t + \phi), \tag{19}$$

where, through standard Laplace transformation analysis,

$$B = |H(j\omega)|A, \tag{20}$$

$$\phi = \angle H(j\omega), \tag{21}$$

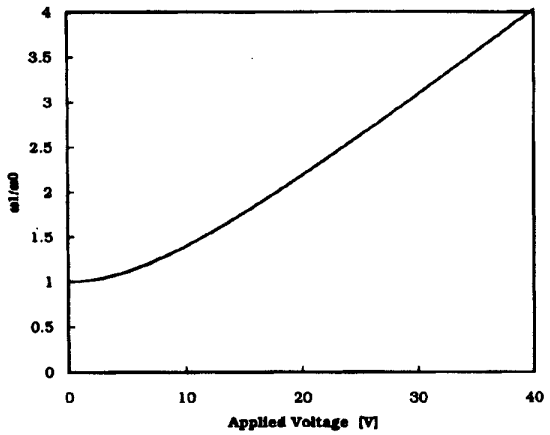

Fig. 6. Theoretical frequency ratio (ω_1/ω_0) versus dc bias (V_P) based on (17), with $\gamma_z = 1.25\ \text{nN}\cdot\text{V}^{-2}$, $k_z = 86\ \text{nN}\cdot\mu\text{m}^{-1}$, and $z_0 = 1.22\ \mu\text{m}$.

and

$$H(j\omega) = \frac{G}{k_{eq} - M\omega^2}. \tag{22}$$

Note that since no damping is assumed, $|H(j\omega)|$ is infinite at $\omega = \omega_1$ and

$$\phi = \begin{cases} 0 & \text{for } \omega < \omega_1 \\ -\pi & \text{for } \omega > \omega_1. \end{cases} \tag{23}$$

In any real system some damping will exist, such that the resonant amplitude is finite, and the phase transition is continuous.

The previous discussion shows that the comb can be used to control the vertical resonance. In the case where the vertical mechanical spring constant of the suspension is very close to the lateral one, i.e., $k_z \approx k_x$, the undesirable simultaneous excitation of both vertical and lateral modes of motion is conveniently avoided, since the dc bias shifts the vertical resonant frequency.

D. Modified Comb Design for Levitation Control

In addition to shifting the vertical resonant frequency, it is desirable to control the dc levitation effect as well. There are several means to reduce the levitation force. By eliminating the ground plane and removing the substrate beneath the structures, the field distribution becomes balanced. Alternatively, a top ground plane suspended above the comb drive will achieve a balanced vertical force on the comb. Both of these approaches require much more complicated fabrication sequences. A simpler solution is to modify the comb drive itself. Reversing the polarity on alternating drive fingers results in the field distribution shown in Fig. 7. In this case, vertical electric fields terminating on the top surface of the movable comb finger are eliminated. To further suppress levitation, the ground plane is modified such that underneath each comb finger there is a strip of conductor biased at the same potential,

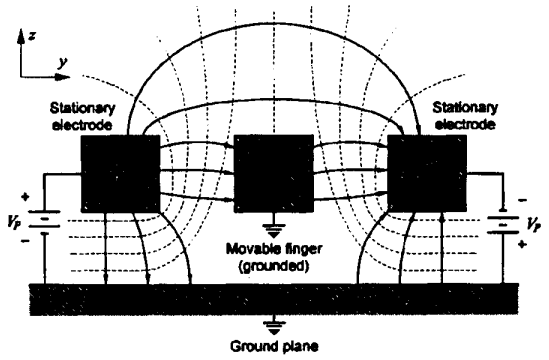

Fig. 7. Cross section of the potential contours (dashed lines) and the electric fields (solid lines) around a movable comb finger when differential dc bias is applied to the two adjacent electrodes.

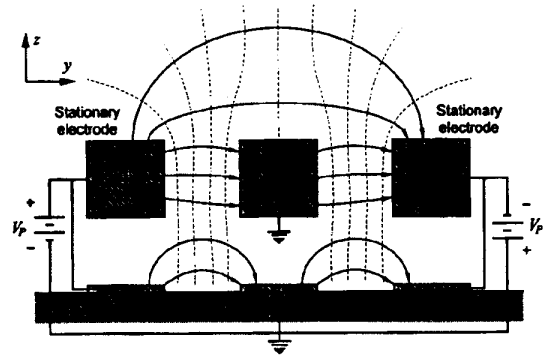

Fig. 8. Cross section of the potential contours (dashed lines) and the electric fields (solid lines) around a movable comb finger when differential dc bias is applied to the two adjacent electrodes and the striped ground conductors.

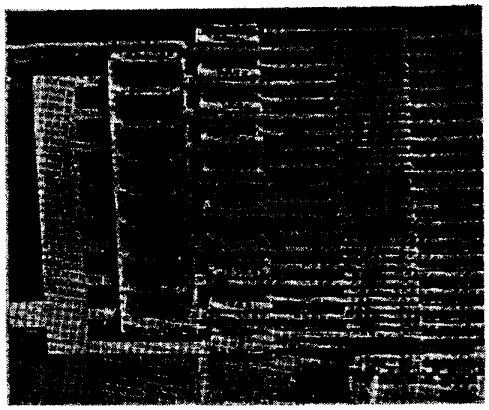

Fig. 9. Scanning electron micrograph (SEM) of the crossover structure for electrical isolation of alternating drive electrodes.

as illustrated in Fig. 8. The polysilicon layer is used to form the crossovers to electrically isolate alternating comb fingers (Fig. 9). Simulation shows that the levitation force

is suppressed by over an order of magnitude compared with the original biasing scheme.

This technique results in a stable system. In contrast, it is difficult to achieve stability if one attempts to counteract the levitation force with an attractive force on the bottom of the movable fingers by driving the underlying electrodes, because of the strong tendency to pull in the fingers and collapsing them to the substrate.

III. Experimental Techniques

Levitation amplitudes are recorded from low-voltage SEM pictures at various dc biases on the combs. All structures are wired together to make possible the measurement of a number of structures in a single SEM session. The angle of tilt and the magnification are fixed for comparison between different structures. Vertical displacements are evaluated by accurately measuring the SEM images with a set of standard line widths. Since the planar geometries of the structures are well defined and the amount of etching undercut of the structural polysilicon can be measured accurately with optical technique, the amount of levitation can be inferred accurately by comparing the dimensions in z with those in x and y. This technique yields an uncertainty level of around 300 Å relative to the planar dimensions, as indicated with the error bars in Figs. 10, 13, and 14. All the prototype devices are designed with 400-μm-long folded-beam supports to provide compliance in both the out-of-plane (z) and the lateral (x) directions. The polysilicon film thickness of the device under test is measured to be 1.94 μm. Due to difficulties with the polysilicon plasma etching process, the cross section of the suspension is slightly trapezoidal, with the width at the top of the beam $a = 2.2$ μm and the width at the bottom $b = 2.8$ μm. The finished comb finger dimensions are 4.2 μm wide on top and 4.8 μm on the bottom, with an overlap length between the finger and the driving electrodes of 20 μm. The gap between the drive electrodes and the comb fingers varies from 1.8 μm near the top surface to 1.2 μm near the bottom. The structures are separated from the substrate by a nominal 2 μm distance, the original thickness of the sacrificial layer. The striped ground planes are similar to those illustrated in Fig. 8, and can be biased accordingly.

The structures are first resonated laterally to evaluate Young's modulus, E, from the measured resonant frequencies using Rayleigh's method [1], [2]. The same value for Young's modulus is then used for the vertical-motion calculations based on the assumption that polysilicon is materially isotropic. The expression for lateral resonant frequency of the test resonator was derived in [3] and [12], with the following result:

$$f_1 = \frac{1}{2\pi}\left(\frac{k_x}{M_p + \frac{1}{4}M_t + \frac{12}{35}M_b}\right)^{1/2} = \frac{1}{2\pi}\left(\frac{24EI_z/L^3}{M_p + \frac{1}{4}M_t + \frac{12}{35}M_b}\right)^{1/2}, \quad (24)$$

where k_x is the lateral spring constant, L is the length of the folded beam (400 μm), M_p is the plate mass, M_t is the mass of the outer connecting trusses, and M_b is beam mass. The moment of inertia of the supporting beams with respect to z (I_z) is given by [13]

$$I_z = \int x^2\,dA = \frac{h}{48}(a + b)(a^2 + b^2). \quad (25)$$

Therefore, E can be expressed as

$$E = \frac{8\pi^2 f_1^2 L^3 (M_p + \frac{1}{4}M_t + \frac{12}{35}M_b)}{h(a + b)(a^2 + b^2)}. \quad (26)$$

Using a polysilicon density of 2.3×10^3 kg·m^{-3}, the value for Young's modulus is found to be 150 GPa for this process run, which is consistent with earlier results [1], [2]. The vertical spring constant is evaluated as

$$k_z = \frac{24EI_x}{L^3} = \frac{2h^3(a^2 + 4ab + b^2)}{3L^3(a + b)}E = 86\ \text{nN}\cdot\mu\text{m}^{-1}. \quad (27)$$

Finally, with this equation, the levitation force can be found as

$$F_z = k_z \Delta z, \quad (28)$$

where Δz is the vertical displacement.

IV. Experimental Results

A. DC Levitation Results

Levitation is first measured by applying a voltage of 0 to 25 V to all drive fingers on a prototype with 18 movable comb fingers and 19 fixed drive fingers, the result of which is plotted in Fig. 10. Fig. 11 is an SEM of a comb structure levitated under a 10 V dc bias. Note that the voltage-contrast effect inside the SEM causes the drive fingers at a higher potential to appear darkened. The vertical displacement increases with applied voltage and reaches an equilibrium near 20 V, where the attractive forces between the displaced interdigitated fingers offset the attractive forces induced on the top surfaces of the movable fingers.

The initial negative deflection for a grounded comb, shown in Fig. 10, cannot be attributed to gravity. With the test chip at a tilt angle of 7° from vertical, the component of the gravitational force normal to the substrate is only 0.09 nN, whereas the force required to cause the initial deflection is 5.9 nN. Nor can there be any built-in stress substantial enough to have caused the deflection. A structure with one of the two anchors deliberately destroyed and thus free of built-in stress showed even more zero-bias deflection inside the SEM. Charging effects in the exposed underlying dielectric films between the interdigitated striped ground plane are a likely source of this offset displacement. With a constant supply of energetic electrons inside the SEM, it is possible that the trap-charge density reaches an equilibrium balanced by the relaxation rate. In order to investigate this hypothesis, we simulated

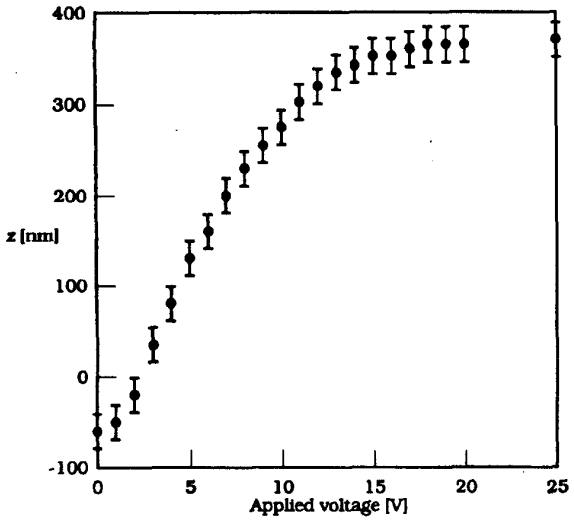

Fig. 10. Measured levitation of an 18-finger comb as a result of applying a common voltage to all drive electrodes.

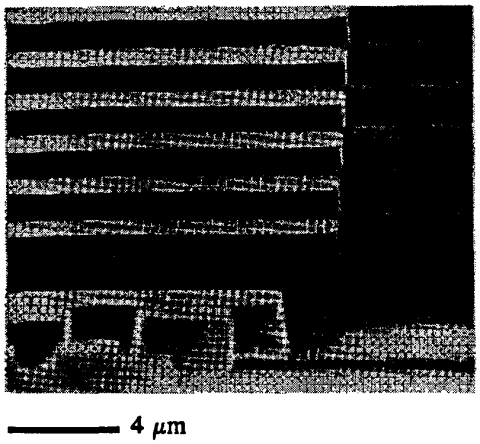

Fig. 11. SEM of an 18-finger comb levitated under 10 V dc bias. Note that the drive fingers, because of the positive bias, appear darkened in the SEM.

the effect of trapped charge in the silicon nitride passivation layer. Figure 12 shows the electric fields and the equipotential contours by assuming an evenly distributed trap-charge density of $-4.3 \times 10^{11}\ q \cdot \mathrm{cm}^{-2}$ inside the 0.15-μm-thick nitride layer, with all the comb fingers, conductors, and the bulk silicon grounded. Simulation results show that this trap-charge density is sufficient to induce the required force on a structure with two 18-finger combs. The magnitude of this charge density is process dependent and is not uncommon for LPCVD nitride films [14]. However, it should be noted that trap charges may also be present in the nitride-oxide interface as well as the thin native oxide layers on the polysilicon ground strips. Furthermore, surface charges on the nitride layer can be either positive or negative, adding complexity to the system. Therefore, the simulated value for the trap-

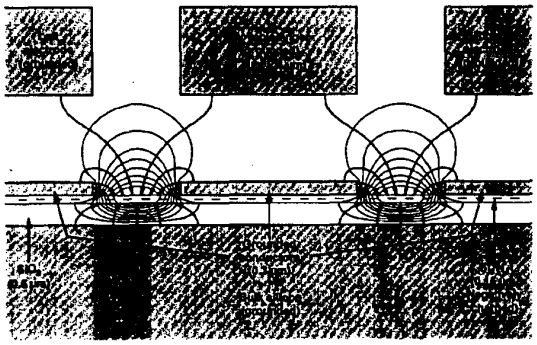

Fig. 12. Cross section of the potential contours (hairlines) and the electric fields (solid lines) of a grounded system with an evenly distributed trapped charge in the silicon nitride layer.

charge density should be treated as a lumped parameter representing the *net* fixed-charge effect. If further investigation is needed, it is possible to verify this initial observation by optical technique, avoiding the undesirable charging inside the SEM.

To account for this trap-charge-induced deflection, we introduce the term F_c as the total trap charge force:

$$F_c = \frac{\beta}{(z + d)^2}, \tag{29}$$

where d is the nominal offset of the structure from the substrate and β is the constant of proportionality, simulated to be 23.6 $\mathrm{nN} \cdot \mu\mathrm{m}^2$. Equation (29) is exact for a layer of trapped charge between a conductor and a ground plane. To account for the partial shielding from the ground strips and fringing-field effects, the power of the denominator in (29) may be adjusted. The term F_c is now added to (4) as

$$F_{\mathrm{net}} = F_z - F_k - F_c = 0. \tag{30}$$

Equations (2) and (5) are combined with (29) to substitute the terms in (30), yielding an implicit function as follows:

$$V_P = \left(\frac{k_z z + \beta/(z + d)^2}{\gamma_z (z_0 - z)/z_0} \right)^{1/2}. \tag{31}$$

Fig. 13 is the result of fitting the curve to the data in Fig. 10 by adjusting z_0 and γ_z. The best-fitted values are $z_0 = 0.4\ \mu\mathrm{m}$ and $z = 1.7\ \mathrm{nN} \cdot \mathrm{V}^{-2}$. The equilibrium levitation (z_0) of 0.4 μm is much less than the observed 2 μm levitation in some structures with soft spring supports and a blanket ground plane. The experimental result for γ_z is comparable to the simulated value of 1.25 $\mathrm{nN} \cdot \mathrm{V}^{-2}$ for an ideal comb structure with 2 μm finger gaps formed with vertical sidewalls.

The effectiveness of levitation control by alternating the potentials on every drive finger is evaluated next. Fig. 14 is a plot of the measured vertical displacement resulting from holding one set of an alternating drive fingers at +15 V and varying the other set of electrodes from −15 V to +15 V. This structure is the same as that tested in Fig.

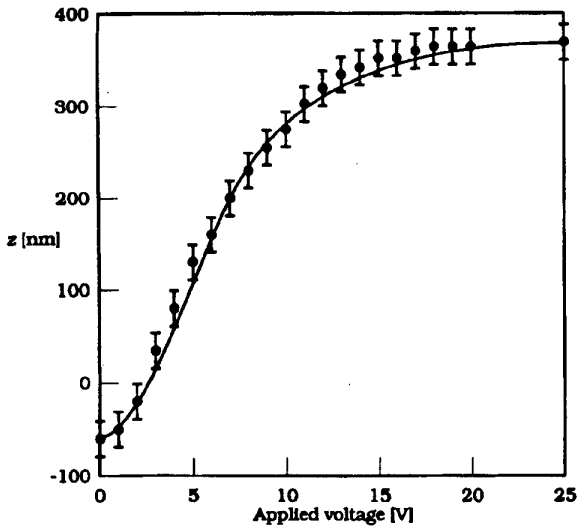

Fig. 13. Measured and calculated levitation of the 18-finger comb.

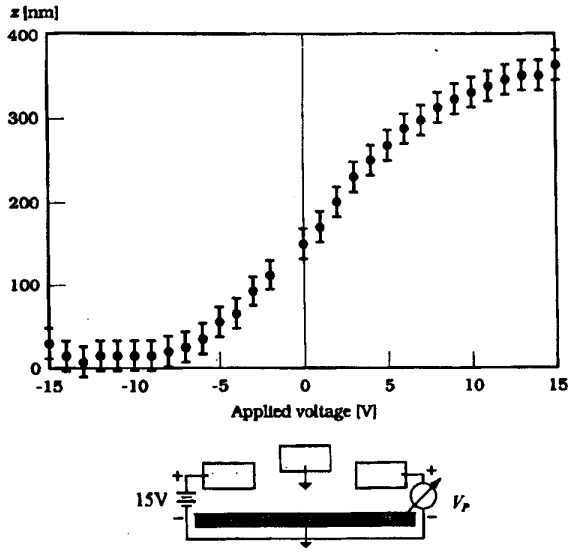

Fig. 14. Measured levitation of the 18-finger comb with the dc bias on one set of electrodes varying from −15 V to +15 V, while the bias on the alternate set is held at +15 V.

10. As expected, negative voltages in the range of −10 V to −15 V suppress the lifting behavior. As the disparity between the magnitudes of the voltages increases, more lifting occurs, with the limiting case of +15 V applied to all drive fingers yielding the same vertical displacement as found in Fig. 10. Fig. 15 is the SEM of a comb structure under a ±10 V balanced biasing on the alternating drive fingers, indicating almost no levitation.

B. Vertical and Lateral Drive Capacities

It is found that, besides suppressing the vertical levitation, the balanced-biasing approach on the alternating

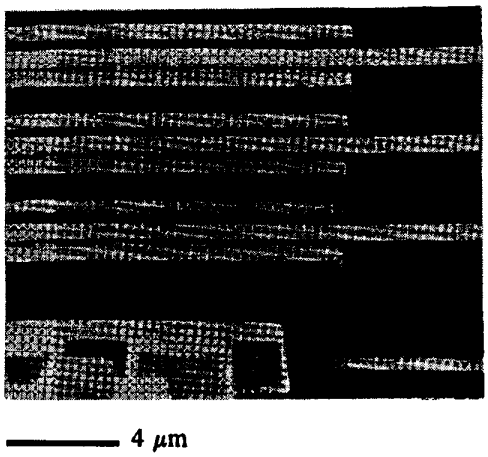

Fig. 15. SEM of an 18-finger comb under ±10 V balanced dc bias on the alternating drive fingers, indicating almost no levitation. Note that fingers at higher potentials appear darkened due to voltage-contrast effect in the SEM.

drive fingers induces a weaker lateral force on the structure than the unbalanced comb. The balanced comb is advantageous only if the trade-off between levitation suppression and loss of lateral drive is favorable. In order to quantify the comparison of the lateral and vertical force reductions, we define the lateral drive capacity, γ_x, of an electrostatic-comb drive as the lateral force (F_x) induced per square of the applied voltage (V_P):

$$\gamma_x = \frac{F_x}{V_P^2} \quad [\text{nN}\cdot\text{V}^{-2}]. \tag{32}$$

The value of γ_x is found to be 0.58 ± 0.04 $\text{nN}\cdot\text{V}^{-2}$ per drive finger for all the unbalanced comb designs. Both γ_x and γ_z for the balanced and unbalanced comb drives are tabulated in Table I. The reductions in γ are defined as the ratios of the drive capacities of the unbalanced comb to those of the balanced one.

Although the balanced-comb design does not completely eliminate the levitation as predicted by idealized theory, which assumes evenly spaced comb fingers with vertical sidewalls, nevertheless a 16:1 reduction on the vertical drive capacity is achieved while suffering only a 1.6:1 reduction in induced lateral force.

C. Vertical Resonant Frequencies and Quality Factors

The vertical resonant frequencies are found by stepping the output frequency of an HP 4192A LF impedance analyzer at 0.1 Hz steps at different dc biases from 5.0 V to 15.0 V, and fixing the ac drive amplitude at 50 mV. Fig. 16 is the SEM of a comb structure driven into vertical resonance under vacuum (10^{-7} torr) inside the SEM chamber. The vibration amplitude is estimated to be 2 μm peak-to-peak. The results are plotted in Fig. 17, with the theoretical curve fitted to the data with z_0 and γ_z adjusted to 0.4 μm and 1.7 $\text{nN}\cdot\text{V}^{-2}$, respectively.

TABLE I
COMPARISON BETWEEN γ_z AND γ_x

Type	γ_z at $z = 0$ ± 0.04 nN·V^{-2}	γ_x ± 0.04 nN·V^{-2}
Unbalanced	1.7	0.58
Balanced	0.11	0.36
Reduction ratio	16:1	1.6:1

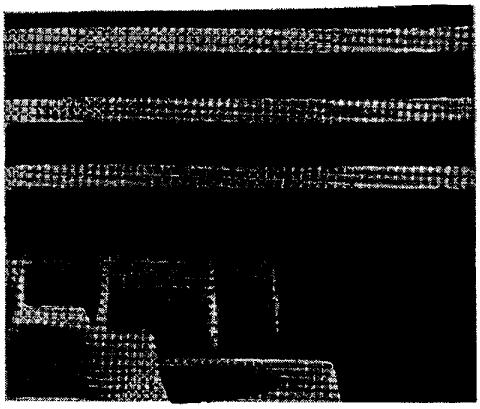

Fig. 16. SEM of an 18-finger comb driven into vertical resonance under a 50 mV ac drive on top of a 5 V dc bias.

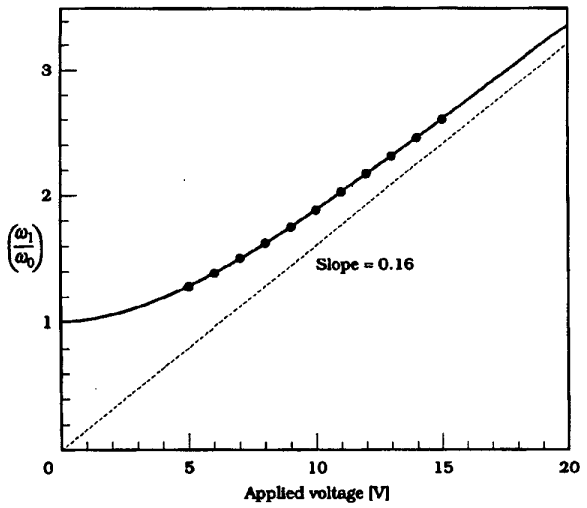

Fig. 17. Measured and fitted vertical resonant frequencies of the 18-finger comb as a function of dc bias. The zero-bias resonant frequency, ω_0, is extrapolated to be 4.69 kHz.

The vertical quality factor, Q, is evaluated using a time-domain method:

$$Q \approx 1.43 \Delta t f_1, \tag{33}$$

where f_1 is the resonant frequency and Δt is the time for the resonance to decay from 90% to 10% of the full amplitude after stopping the drive. The Q for all the structures tested in vacuum is close to 50 000, which is the same as the lateral Q in vacuum. However, it is found that vertical resonance can be excited over a range of ± 10 Hz of the resonant frequencies, which, if the system were linear, would have put the values for Q in the range of 250 to 500. This apparently excessive ± 3 dB bandwidth may be due to the highly nonlinear function of vertical resonant frequency on the drive voltage. Since the vertical position is also a function of the applied voltage, the large vibration amplitude of 2 μm peak-to-peak indicates that the vertical resonance is in the nonlinear region even at an ac drive level of 50 mV. Nevertheless, the excellent fit of the linear theory with the experimental results verifies the usefulness of the frequency-shifting phenomenon as a way to control vertical resonant frequency.

V. CONCLUSIONS

We have successfully modeled and experimentally investigated both dc and ac levitation induced by electrostatic-comb drives by direct tests in an SEM, which provides insights into designing structures for controlled out-of-plane motions. The best levitation suppression is obtained by alternating the electrodes at every comb finger with a striped ground plane underneath the comb structure. Levitation can be further reduced by designing structures with vertically stiff suspensions. If controlled levitation is desired, soft suspensions can be used together with ratioed differential and common mode voltages applied to the two electrodes. Decoupling of vertical and lateral resonant modes can be achieved by simply applying a dc bias to the drive electrodes.

ACKNOWLEDGMENT

The authors wish to thank C. Hsu and the staff at the Berkeley Microfabrication Laboratory for their assistance in the fabrication process. The discussions on dielectric trap charges with Prof. J. Chung (Massachusetts Institute of Technology) and Prof. M. Aslam (Michigan State University) are gratefully acknowledged.

REFERENCES

[1] W. C. Tang, T.-C. H. Nguyen, and R. T. Howe, "Laterally driven polysilicon resonant microstructures," *Sensors and Actuators*, vol. 20, pp. 25-32, 1989.

[2] W. C. Tang, T.-C. Nguyen, M. W. Judy, and R. T. Howe, "Electrostatic-comb drive of lateral polysilicon resonators," in *Proc. 5th Int. Conf. Solid-State Sensors and Actuators (Transducers '89)* (Montreux), vol. 2, June 25-30 1989, pp. 328-331.

[3] W. C. Tang, "Electrostatic comb drive for resonant sensor and actuator applications," Ph.D. thesis, Dept. EECS, Univ. California, Berkeley, Dec. 1990.

[4] R. A. Brennen, A. P. Pisano, and W. C. Tang, "Multiple mode micromechanical resonators," in *Proc. IEEE Micro Electro Mech. Syst. Workshop* (Napa Valley, CA), Feb. 1990, pp. 9-14.

[5] M. G. Lim, J. C. Chang, D. P. Schultz, R. T. Howe, and R. M. White, "Polysilicon microstructures to characterize static friction," in *Proc. IEEE Micro Electro Mech. Syst. Workshop* (Napa Valley, CA), Feb. 1990, pp. 82-88.

[6] C.-J. Kim, A. P. Pisano, R. S. Muller, and M. G. Lim, "Polysilicon microgripper," in *Tech. Dig. IEEE Solid-State Sensor and Actuator Workshop* (Hilton Head, SC), June 1990, pp. 48-51.

[7] W. Yun, R. T. Howe, and P. R. Gray, "Surface micromachined, digitally force-balanced accelerometer with integrated CMOS detection circuitry," in *Tech. Dig. IEEE Solid-State Sensor and Actuator Workshop* (Hilton Head, SC), June 1992, pp. 126–131.
[8] A. P. Pisano, "Resonant-structure micromotors," in *Proc. IEEE Micro Electro Mech. Syst. Workshop* (Salt Lake City, UT), Feb. 1989, pp. 44–48.
[9] Y.-C. Tai, L.-S. Fan, and R. S. Muller, "IC-processed micro-motors: design, technology and testing," in *Proc. IEEE Micro Electro Mech. Syst. Workshop* (Salt Lake City, UT), Feb. 1989, pp. 1–6.
[10] M. Mehregany, P. Nagarkar, S. D. Senturia, and J. H. Lang, "Operation of microfabricated harmonic and ordinary side-drive motors," in *Proc. IEEE Micro Electro Mech. Syst. Workshop* (Napa Valley, CA), Feb. 1990, pp. 1–8.
[11] Ansoft Corp., 4 Station Square, 660 Commerce Court Bldg., Pittsburgh, PA, Maxwell Solver, Electrostatic Package.
[12] W. C. Tang, M. G. Lim, and R. T. Howe, "Electrostatically balanced comb drive for controlled levitation," in *Tech. Dig. IEEE Solid-State Sensor and Actuator Workshop* (Hilton Head, SC), June 1990, pp. 23–27.
[13] J. M. Gere and S. P. Timoshenko, *Mechanics of Materials*, 2nd ed. Belmont: Wadsworth, 1984.
[14] S. M. Sze, *Physics of Semiconductor Devices*, 2nd ed. New York: John Wiley, 1981.

William C. Tang (S'86–M'90) received the Ph.D. degree in electrical engineering from the University of California at Berkeley in 1990.

He was an associate engineer/scientist at the General Products Division, IBM Corp., from 1982 to 1984. He is currently a senior research engineer at the Ford Research Laboratory, Ford Motor Company, Dearborn, MI. His primary responsibilities include research in micromachining technology and automotive applications of micromechanics. Dr. Tang is a member of the Materials Research Society.

Martin G. Lim received the B.S.M.E. degree in 1987 from the University of California at Berkeley. Later he joined the Berkeley Sensor and Actuator Center and completed his M.S. in 1990.

He is currently a member of the research staff at Xerox Palo Alto Research Center working on acoustic ink printing. His responsibilities include research and development in micromechanical systems and their fabrication processes.

Roger T. Howe (S'80–M'84) received the Ph.D. degree in electrical engineering from the University of California at Berkeley in 1984.

He was on the faculty of Carnegie-Mellon University from 1984 to 1985 and was an assistant professor at the Massachusetts Institute of Technology from 1985 to 1987. In 1987, he joined the Department of Electrical Engineering and Computer Sciences at the University of California at Berkeley, where he is now an associate professor and an associate director of the Berkeley Sensor and Actuator Center. His research interests include resonant microsensors and microactuators, micromachining technology, and integrated-circuit design.

Prof. Howe is a member of the Materials Research Society, the Electrochemical Society, and Sigma Xi.